Gyrokinetic Electrostatic Simulations of Drift Modes in Dipole Configuration

Hua-sheng XIE[1] (谢华生)
huashengxie@{gmail.com, pku.edu.cn}, http://hsxie.me

[1]Fusion Simulation Center, School of Physics, State Key Laboratory of Nuclear Physics and Technology, Peking University, Beijing 100871, China

Sherwood Fusion Theory Conference, May 1-3, 2017, Annapolis, MD - USA

Team at PKU: Bo LI (李博), Wei-ke OU (欧伟科), Yi ZHANG (张铱), Zi-cong HUANG (黄子瑰).

Ackn.: J. Kesner (MIT), B. Rogers (Dartmouth), M. Mauel (Columbia), P. Porazik (PPPL&UCI), Y. Y. Li (李跃岩, ZJU), Z. Lin (UCI&PKU), · · ·

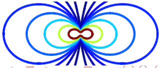

Two goals: magnetic confinement fusion (Hasegawa1987) & space environment

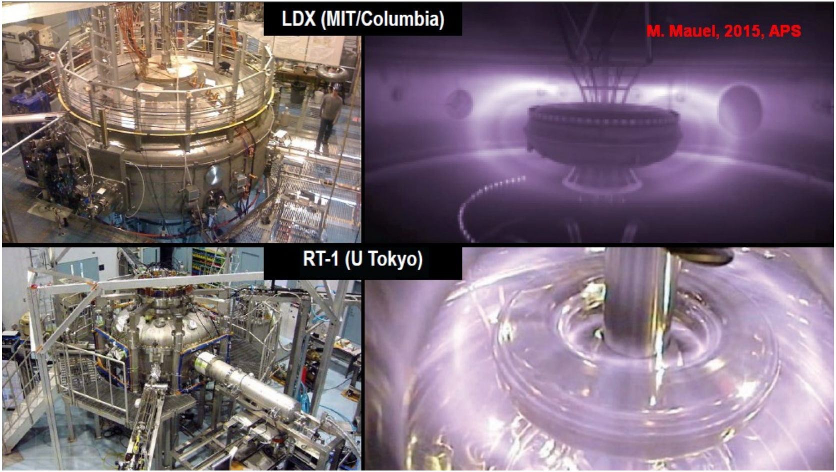

Laboratory dipole, LDX (MIT), CTX(Columbia) and RT-1 (Tokyo). Also, HDX: ∼￥2B, Harbin, China.

For magnetic confinement fusion (Hasegawa1987)

Does magnetospheric physics apply to magnetic confinement in the laboratory?

Mauel15APS

- ***Levitate*** a small, high-current superconducting current ring within a very large vacuum vessel
- ***Inject*** heating power and a source of plasma particles at outer edge (SOL)
- ***Somehow drive*** low-frequency fluctuations that create radial transport, preserve (μ, J), and sustain "centrally-peaked" profiles at marginal stability
- ***Achieve*** high beta, $\beta \geq 1$, steady-state, and link space and fusion studies

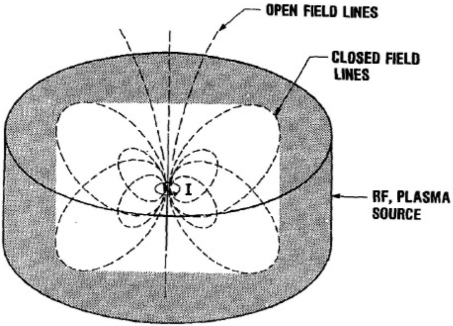

Akira Hasegawa, *Comments on Plasma Physics and Controlled Fusion* **11**, 147 (1987)

Motivation of building LDX.

Perfect confinement of charged particles in ideal magnetic dipole field, $\mathbf{F} = \mathbf{v} \times \mathbf{B}$, $\mathbf{B}(r) = \nabla\Psi(\mathbf{r})$, $\Psi(\mathbf{r}) = \frac{\mu_0}{4\pi r^3}\mathbf{M}\cdot\mathbf{r} = \frac{\mu_0}{4\pi r^2}\mathbf{M}\cdot\hat{\mathbf{r}}$.

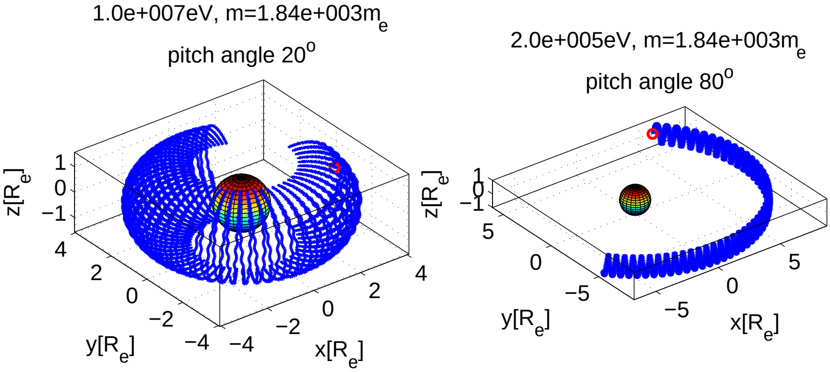

Collision and turbulence lead transport. Two major (electrostatic) instabilities: interchange and entropy[1] modes. Driven by gradients (∇T and ∇n).

[1] More accurate: electrostatic drift mode.

1. Gyrokinetic-Poisson equations to solve

- 3D nonlinear

$$\frac{d}{dt}f_\alpha(\mathbf{X},\mu,v_\|,t) = \left[\frac{\partial}{\partial t}+\dot{\mathbf{X}}\cdot\bar{\nabla}+\dot{v}_\|\frac{\partial}{\partial v_\|}\right]f_\alpha = C_\alpha f_\alpha, \quad (1)$$

$$\frac{\tau}{\lambda_D^2}(\Phi-\tilde{\Phi}) = 4\pi e(\bar{n}_i-n_e), \quad (2)$$

$$\dot{\mathbf{X}} = v_\|\mathbf{b}+\mathbf{v}_E+\mathbf{v}_d, \qquad \mathbf{v}_E = \frac{\mathbf{b}\times\nabla\bar{\Phi}}{B}. \quad (3)$$

- 1D linear

$$f_j = -\frac{q_j}{T_j}F_{0j}\phi+J_0(k_\perp\rho)h_j, \quad (4)$$

$$(\omega-\Omega_d+iv_\|\partial_\|)h = -(\omega-\Omega_*)q\phi\frac{\partial F_0}{\partial\epsilon}J_0(k_\perp\rho), \quad (5)$$

$$\int f_i dv^3 = \int f_e dv^3. \quad (6)$$

$\mathbf{B} = \nabla\phi \times \nabla\psi_p$, $\psi_p = \frac{M}{r}\sin^2\theta$. Flux coordinates (χ, ψ, ζ) can be $\chi = \theta$, $\psi = \frac{M\sin^2\theta}{r}$, $\zeta = \phi$. Flux surface

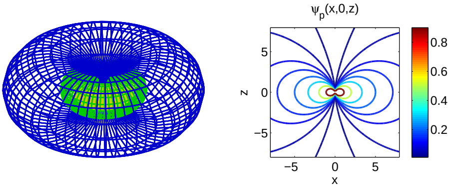

coordinate grids

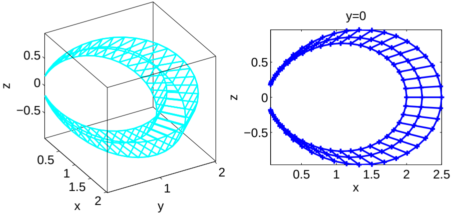

To save the computation cost by using the symmetries.

- Gyrokinetic equation

$$\frac{d}{dt}f_\alpha(\mathbf{X},\mu,v_\parallel,t)=\left[\frac{\partial}{\partial t}+\dot{\mathbf{X}}\cdot\bar{\nabla}+\dot{v_\parallel}\frac{\partial}{\partial v_\parallel}\right]f_\alpha=C_\alpha f_\alpha. \quad (7)$$

- Guiding center (GC) phase space coordinates $(\chi,\psi,\zeta,v_\parallel,\mu,\xi)$. GC Lagrangian

$$L=\frac{e}{c}\Big\{(\psi+\delta A_\zeta)\dot{\zeta}+(\alpha+\frac{v_\parallel}{\Omega})B_\chi\dot{\chi}+[(\alpha+\frac{v_\parallel}{\Omega})B_\psi+\delta A_\psi]\dot{\psi}\Big\}+\frac{mc}{e}\mu\dot{\xi}-\mu B-\frac{1}{2}mv_\parallel^2-e\Phi, \quad (8)$$

$\Omega=eB/mc$, $\mu=mv_\perp^2/(2B)$. For equations of motion, $\dot{\mu}=0$ and $\dot{\xi}=eB/mc$.

- Electrostatic $\delta\Phi=\delta\Phi(\chi,\psi,\zeta)$, $\delta\mathbf{B}=0$

$$\dot{\chi} = \frac{1}{B_\chi}[cB_\psi\partial_\zeta\Phi+v_\parallel B], \quad (9)$$

$$\dot{\psi} = -\left(\frac{c}{e}\right)e\partial_\zeta\Phi, \quad (10)$$

$$\dot{\zeta} = \left(\frac{c}{e}\right)\left(\partial_\psi-\frac{B_\psi}{B_\chi}\partial_\chi\right)(\mu B+e\Phi)+\frac{v_\parallel^2}{\Omega}\left(\partial_\psi-\frac{B_\psi}{B_\chi}\partial_\chi\right)B, \quad (11)$$

$$\dot{v_\parallel} = -\Omega\left[\frac{v_\parallel}{\Omega}\frac{1}{B}\left(\frac{c}{e}\right)(e\partial_\zeta\Phi)\left(\partial_\psi-\frac{B_\psi}{B_\chi}\partial_\chi\right)B+\left(\frac{c}{e}\right)\frac{1}{B_\chi}\partial_\chi(\mu B+e\Phi)\right]. \quad (12)$$

Particle-in-cell

- Interpolation between particles (makers) (χ, ψ, ζ) to grids $(\chi_i, \psi_j, \zeta_k)$

Weight

$$W = \frac{\int_{\chi}^{\chi_{i+1}} \int_{\psi}^{\psi_{j+1}} \int_{\zeta}^{\zeta_{k+1}} J d\chi d\psi d\zeta}{\int_{\chi_i}^{\chi_{i+1}} \int_{\psi_j}^{\psi_{j+1}} \int_{\zeta_k}^{\zeta_{k+1}} J d\chi d\psi d\zeta}$$

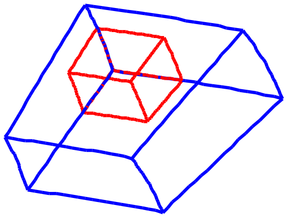

$$W = W_\chi W_\psi W_\zeta = \left(1 - \frac{\int_{\chi_i}^{\chi} \sin^7 \chi d\chi}{\int_{\chi_i}^{\chi_{i+1}} \sin^7 \chi d\chi}\right)\left(1 - \frac{1/\psi_j^3 - 1/\psi^3}{1/\psi_j^3 - 1/\psi_{j+1}^3}\right)\left(1 - \frac{\zeta - \zeta_k}{\zeta_{k+1} - \zeta_k}\right).$$

- δf method to reduce noise
  $\frac{dw}{dt} = -(1-w)\frac{df_0}{f_0 dt}$, $w = \delta f / f$
- Initial Maxwellian $f_0 = \frac{1}{\sqrt{2\pi}} \exp\left(-\frac{v_\parallel^2 + v_\perp^2}{2}\right) v_\perp$, $\mu = 2v_\perp^2/B$

Simple test case: IAW. Adiabatic electron $\delta n_e = e\delta\phi/T_e$, quasi-neutrality $\delta n_i = \delta n_e$, thus:

$$\frac{1}{\tau} e\delta\phi/T_i = \delta n_i = \int \delta f_i dv, \quad (\tau = T_e/T_i). \tag{13}$$

Slab limit (ES1D) dispersion relation

$$D(\omega, k) = 1 - \frac{\tau}{2} Z'(\zeta_i), \tag{14}$$

$Z'(\zeta) = -2(1+\zeta Z)$, $\zeta_i = \omega/k_{\|} v_{ti}$.

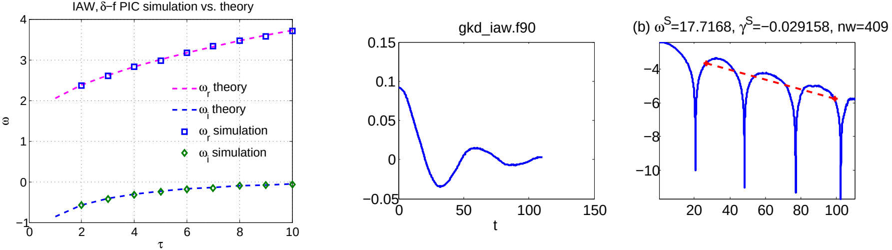

We have built the framework for 3D nonlinear simulation (code name: GKD), but only tested uniform IAW at this stage. Future works: 3D drift modes.

2. Linear 0D dispersion relation[2]

Dipole or Z-pinch, safety factor and shear $q = s = 0$, simpler than tokamak. For simplicity, also $k_{||} = 0$ and $k_r = 0$, i.e., $k = k_\perp$.

$$D(\omega, k) = \sum_\alpha \frac{1}{T_\alpha}\left\{1 - \int dv^3 \frac{[\omega - \Omega_*(v)]J_0\langle J_0(k_\perp \rho)\rangle_b F(v)}{[\omega - \langle \Omega_d(v)\rangle_b]}\right\} = 0. \quad (15)$$

The only difference between dipole and Z-pinch [Ricci06] is the bounce average terms $\langle J_0\rangle_b$ and $\langle \Omega_d\rangle_b$, with $\langle\cdot\rangle_b = \oint \cdot dl/v_{||}$.

With Maxwellian F_0, after normalization by v_{ti}/R and add $k_{||}$ term

$$D(\omega, k) = \sum_\alpha \frac{1}{T_\alpha}\left\{1 - \frac{1}{\sqrt{2\pi}}\int \frac{[\omega - \Omega_*(y)]J_0 J_{0b}(k_\alpha y_\perp)}{[\omega - k_{z\alpha} y_{||} - \Omega_{db}(y)]} e^{-\frac{y^2}{2}} y_\perp dy_\perp dy_{||}\right\} = 0. \quad (16)$$

$\Omega_{*\alpha} = \omega_{d\alpha}[\kappa_n + \kappa_T(y^2/2 - 3/2)]$, $\kappa_n = L_n^{-1}R$, $L_n^{-1} = -d\ln n/dr$, $k_{zi} = k_{||}R$, $k_{ze} = k_{||}R\sqrt{\tau m_i/m_e}$, $\omega_{di} = k$, $\omega_{de} = k\tau q_i/q_e$, $k_i = k$, $k_e = k\frac{q_i}{q_e}\sqrt{\tau m_e/m_i}$, $y^2 = y_{||}^2 + y_\perp^2$, $\Omega_d = \omega_{d\alpha}(y_{||}^2 + y_\perp^2/2)$.

Note: dipole, Ω_d should be Ω_{db} & $\omega_{di} = 3k$ due to the curvature radius $R_c = R/3$.

[2] Numerical approaches: H. S. Xie, Y. Y. Li, Z. X. Lu, W. K. Ou and B. Li, Comparisons and Applications of Four Independent Numerical Approaches for Linear Gyrokinetic Drift Modes, 2017, submitted to PoP.

Curvature stabilize the mode, bounce average Ω_d destabilize the solution

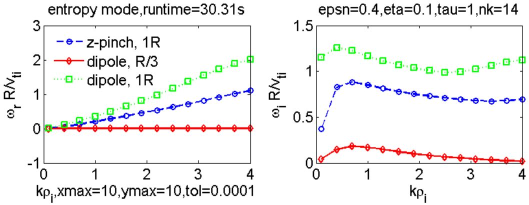

Bounce average of J_0 change the solution quantitatively

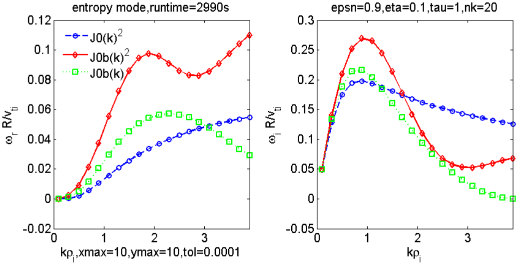

Thus, curvature radius $R \to R/3$ is the most important effect.

Two branches, $\eta \equiv \kappa_T/\kappa_n \lessapprox 0.7$ similar to electron drift mode, $\eta \gtrapprox 0.7$ similar to ion temperature gradient (ITG) mode

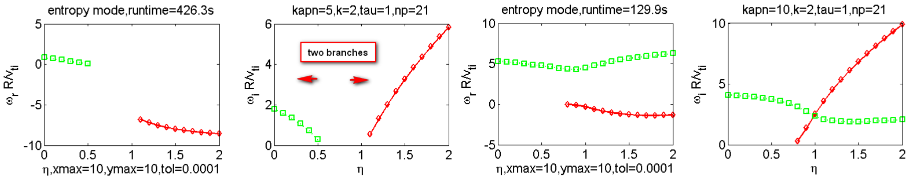

The nonlinear physics of these two branches are very different. See later.

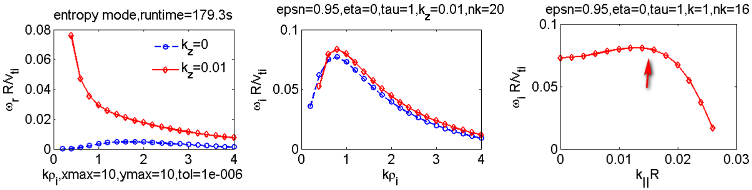

The most unstable mode is $k_{\|} R \sim 0.015 \neq 0$.

Interchange-like mode ($\epsilon_n = 0.2,\ k \to 0,\ \gamma \to \gamma_0 \neq 0$) vs entropy-like mode ($\epsilon_n = 0.5,\ k \to 0,\ \gamma \to 0$)

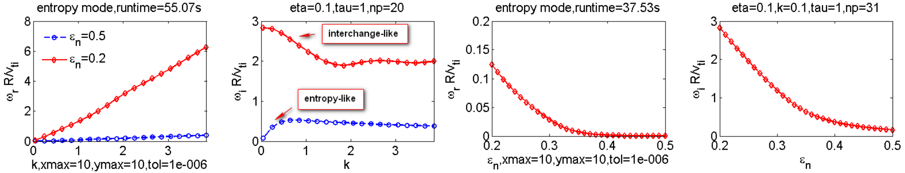

Collision $[C(g_e) = \hat{\nu}_e(v)\frac{\partial}{\partial\xi}(1-\xi^2)\frac{\partial g_e}{\partial\xi},\ \xi = v_\parallel/v]$ slightly stabilize the mode (via initial value simulation)

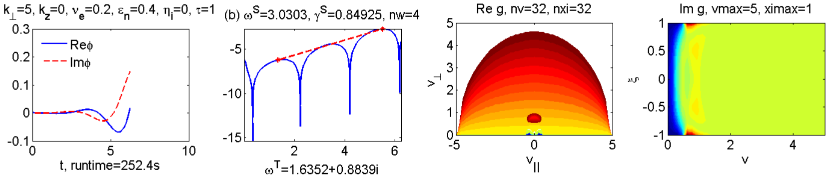

$\nu_e = 0 \to 0.2,\ \omega = 1.64 + 0.88i \to 1.51 + 0.85i$

3. Linear 1D PIC simulation

The gyrokinetic system

$$\frac{d\xi}{dt} = \frac{v_\parallel}{\kappa}, \tag{17}$$

$$\frac{dw}{dt} = -i\omega_{Ds}w - i(\omega_{Ds} - \omega_{*s}^T)\frac{q_s}{T_s}J_0\phi - v_\parallel \frac{1}{\kappa}\frac{q_s}{T_s}[J_0\partial_\xi\phi - J_1\partial_\xi(k_\perp\rho_s)\phi], \tag{18}$$

$$\left(1 + \frac{1}{\tau_e} - \Gamma_{0i} - \frac{1}{\tau_e}\Gamma_{0e}\right)\phi = \int J_{0i}g_i d^3v - \int J_{0e}g_e d^3v. \tag{19}$$

To avoid the $\pm v_\parallel$ of treating the turning point, we add a new equation to calculate $v_\parallel$

$$\frac{dv_\parallel}{dt} = -\frac{v^2\lambda}{2r_0}\frac{1}{\kappa}\frac{df}{d\xi} \to -\frac{v^2\lambda}{2}\frac{1}{\kappa}\frac{df}{d\xi}. \tag{20}$$

$w = g/F_0$ is δf particle weight. $\xi = \theta - \pi/2$ (point dipole) or $\xi = \theta$ (ring dipole) is the field line coordinate.

To understand:

- passing particles (z-pinch) vs trapped particles (dipole)
- $s = 0$ vs $s \neq 0$ (tokamak)

Typical current loop/ring dipole configuration parameters

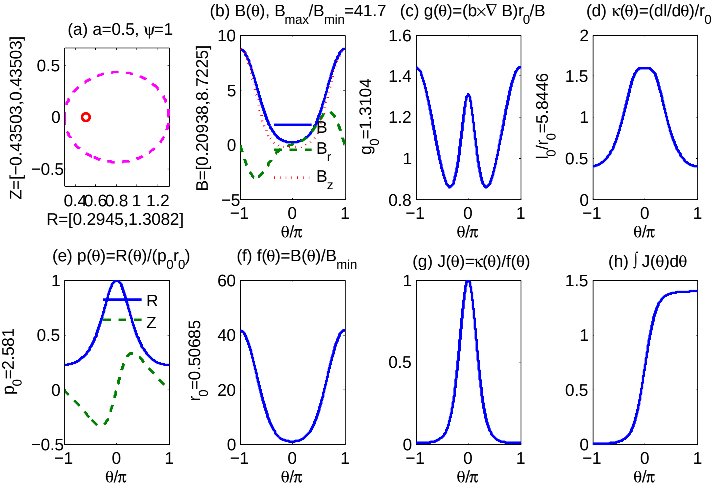

The above field line dynamic model can also be easily used to other configurations such as FRC and tokamak under s-α ballooning space.

Distribution function $F(\theta, v_{\|}, v_{\perp}, t) = F(\theta, v_{\|}, v_{\perp}, t=0) = F_M$

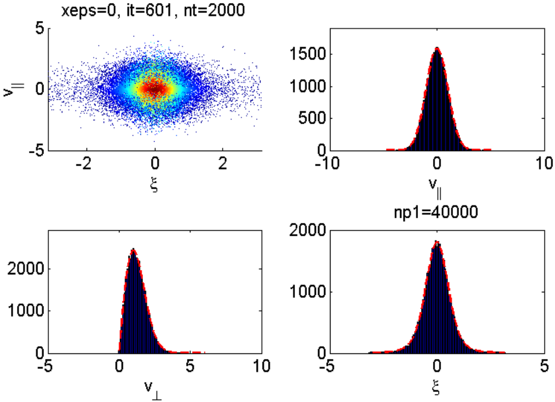

Note: Initial loading $F(\theta) \propto J(\theta) = \kappa(\theta)/f(\theta)$.

Scan $k_\perp \rho_i$ (gkd1d code, f90 + mpi)

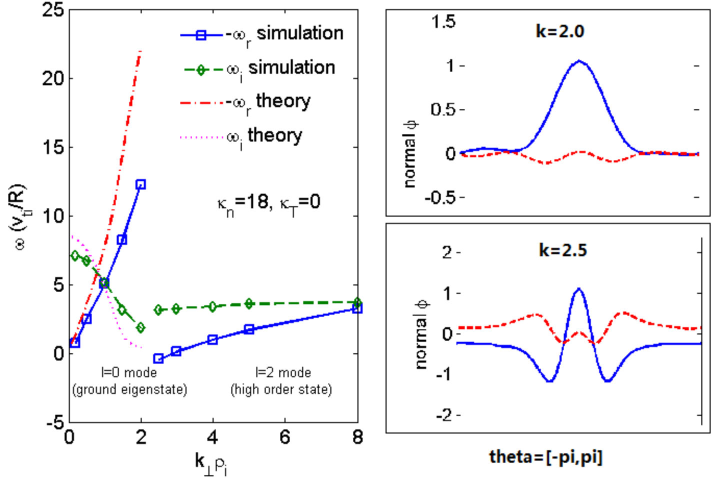

Against to previous result of $k_\parallel \sim 0$ mode dominate, a high order $k_\parallel \neq 0$ mode is most unstable at larger $k_\perp \rho_i$ for strong gradient $\kappa_n = 18$. New!!

4. Preliminary nonlinear results

At small $k_\perp$ limit, $\Gamma_0 = 1 - b_i$, $b_i \rightarrow \nabla_\perp^2$. Gyrokinetic Poisson equation becomes $\nabla_\perp^2 \delta\phi = \delta n_e - \delta n_i$.

$\hat{\mathbf{b}} = \hat{\mathbf{z}} + \theta\hat{\mathbf{y}}$, $\theta \ll 1$, in 1D limit, we solve

$$\begin{aligned} & \partial_t \delta f + \theta v_\parallel \partial_y \delta f - \alpha\theta\partial_y\phi\partial_{v_\parallel}\delta f \\ = & -[\kappa_n + \kappa_T(v_\parallel^2/2v_t^2 - 1/2)]\partial_y\phi f_0 - \alpha\theta\partial_y\phi(v_\parallel/v_t^2)f_0, \end{aligned} \tag{21}$$

$$\partial_{yy}\delta\phi = \delta n_e - \delta n_i. \tag{22}$$

The $E \times B$ nonlinearity is omitted, only keep parallel nonlinearity. For simplification, only ω_*, no ω_d.

The model similar to Parker&Lee1993, but include κ_T.

$\eta < 1$ branch, parallel nonlinearity can lead saturation

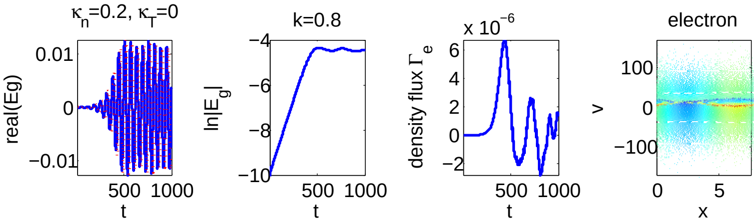

$\eta > 1$ branch, parallel nonlinearity cannot lead saturation

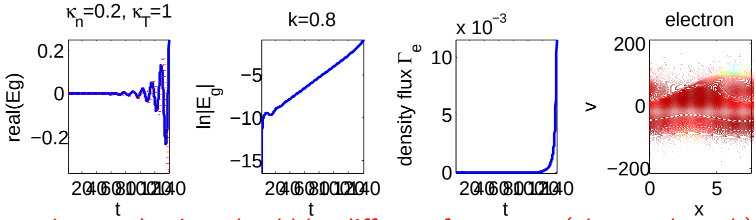

The saturation mechanism should be different for $\eta < \eta_c$ (electron branch) and $\eta > \eta_c$ (ion branch) branches.

Backup

Linear physics in (κ_n, κ_T) space

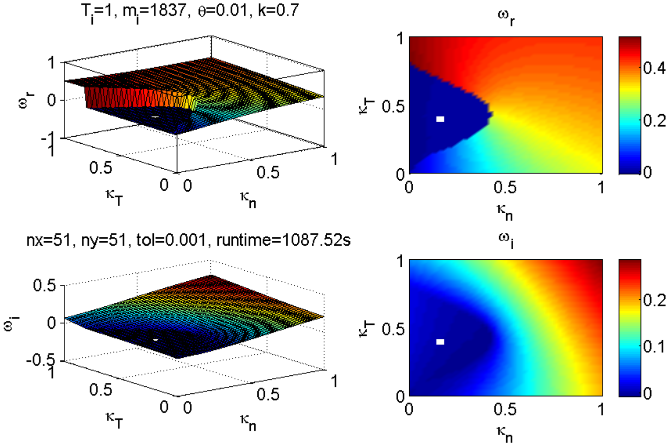

Physics can be different for different density and temperature gradients.